

## Numerical solution of the spatially inhomogeneous Boltzmann equation and verification of the nonlocal approach for an argon plasma

C. Busch and U. Kortshagen

*Institut für Experimentalphysik II, Ruhr-Universität Bochum, D-44780 Bochum, Germany*

(Received 2 September 1994)

The spatially dependent description of the electron kinetics is of vital interest for the modeling of complete plasma devices. A possible method of dealing with this problem is by the solution of the Boltzmann equation accounting for the spatial inhomogeneity. This approach can be a complicated task. On the other hand, this method may be much more efficient than the treatment of the electron kinetics by simulation techniques. In this paper, the numerical solution of the spatially dependent Boltzmann equation for an argon plasma in cylindrical geometry is reported. A detailed discussion on the boundary conditions is presented. The numerical results are compared to results of the “nonlocal approach,” which is a very efficient method for the solution of the spatially dependent Boltzmann equation for the limiting case that the energy relaxation length of electrons exceeds the discharge dimensions. The range of applicability of the nonlocal approach is discussed in terms of the neutral gas density and the inhomogeneity of the electric field.

PACS number(s): 51.10.+y

### I. INTRODUCTION

Due to the growing number of applications of gas discharges their modeling has attracted increasing interest in recent years (see, e.g., Ref. [1]) for mainly two reasons. First, self-consistent plasma models or numerical experiments can help to understand the basic physical properties of concrete plasma devices, and secondly they can serve as a tool or guide for the discharge construction. In these models the spatially dependent description of the electron kinetics plays a central role. The electron distribution function (EDF) determines the electron induced reactions in the plasma, e.g., the ionization, excitation, or dissociation. It thus strongly influences also the macroscopic properties of the plasma, like the electron density profile or the spatial distribution of fluxes of charged particles, neutral species, and radicals. The knowledge of the EDF and of its spatial dependence is thus a basic requirement for self-consistent plasma models.

Quite complete models have been proposed in recent times, e.g., for the capacitively or the inductively coupled rf discharge [2–8]. These models, which consist of various modules for determining the EDF, the space charge potential, the rf field profile, etc., yield quite accurate results but are, on the other hand, computationally tedious. The electron kinetics part is usually particularly computer intensive and is frequently treated by simulation techniques [2,4,9] or by numerical [10–12] integration of the Boltzmann equation. However, it is surely desirable to develop fast and efficient models which allow one to perform scans over wide parameter ranges, if possible, on simple and easily available computers. The formulation of efficient approaches to the description of the spatially dependent electron kinetics is thus an interesting and promising task.

A considerable reduction of computational work and

a gain of physical insight may be achieved under conditions where the Boltzmann equation can be solved using some well-studied approximations. In cases when the anisotropy of the EDF is small (no considerable influence of high energetic secondary electrons and elastic collisions are frequent in comparison to inelastic ones), the usual two-term approximation for the EDF is applicable [13]. For a dc or a hf electric field of sufficiently high frequency, the isotropic part of the EDF is time independent [14]. Employing these approximations, the resultant kinetic equation for the isotropic part of the EDF comprises, apart from one dimension in velocity or energy space, still one or more dimensions in configuration space. Numerical solutions of problems of this kind have been reported recently [15–17]. However, the numerical solution of the spatially dependent kinetic equation, resulting from these approximations, remains still a complicated task.

A simplification of the problem has been proposed by Bernstein and Holstein [18] and Tsengin [19]. Their method, the so-called “nonlocal approach,” relies on the assumption that the entire electron kinetics can be described by a single, spatially homogeneous distribution function of *total energy* (i.e., kinetic plus potential energy) of the electrons which is determined from a spatially averaged kinetic equation. The *spatially resolved* EDF of kinetic energy can then be calculated from a sort of “modified Boltzmann relation.” The validity of the nonlocal approach is limited to conditions where the energy relaxation length of electrons exceeds the typical discharge dimensions. Then the spatial redistribution of energy gains and losses due to the rapid spatial motion of electrons justifies the determination of the EDF from a spatially averaged kinetic equation. The qualitative validity of this approach has been demonstrated in a number of investigations [20–22]. By comparison between spatially resolved measurements of the EDF in a surface wave plasma and a self-consistent plasma model based on the nonlocal approach, even quantitative agreement

has been demonstrated recently [23]. The value of the nonlocal approach for plasma modeling is obvious. Since the EDF is determined from a one-dimensional, spatially averaged kinetic equation, the dimensionality of the electron kinetics is always reduced to one energy dimension regardless of the number of spatial dimensions to be considered.

In a number of publications it has been demonstrated that the nonlocal approach can be used as a powerful tool for plasma modeling [23–26]. Thus a demonstration of its quantitative accuracy is highly important. However, up to now a numerical verification of the nonlocal approach as well as a detailed discussion on its range of applicability is still missing. In particular, the discussion of the limits of applicability are mostly based on more or less qualitative arguments which deserve a more quantitative investigation. It is the purpose of this paper to investigate the validity of the nonlocal approach by comparison with numerical solutions of the spatially dependent Boltzmann equation.

## II. BOLTZMANN EQUATION ANALYSIS OF THE SPATIALLY DEPENDENT ELECTRON KINETICS

### A. Kinetic equations

The situation addressed is that of a positive column. The plasma is maintained by a temporally and spatially constant axial electric field  $\mathbf{E}_z$ . The electron confining space charge electric field  $\mathbf{E}_t \parallel \nabla n_e$  is directed radially. For the purpose of the present discussion a self-consistent formulation of the problem is not necessary. Thus we restrict ourself to a parametric model. The ambipolar potential which is connected to the transverse electric field  $\mathbf{E}_t$  is assumed to be parabolic:  $\Phi(r) = \Phi_{sh}(r/R)^2$ . In the present discussion, we assume a fixed value of the potential  $\Phi_{sh}$  at the plasma-sheath boundary of  $-8$  V.

The Boltzmann equation is simplified by employing the well-known two-term approximation. Usually a formulation in kinetic energy  $u = mv^2/(2e)$  in volts is chosen:

$$F(u, r) = F_0(u, r) + \frac{\mathbf{v}}{v} \cdot \mathbf{F}_1(u, r). \quad (1)$$

Employing this approximation one obtains after some algebra which is well documented in a number of textbooks (e.g., [27]), a kinetic equation for the isotropic part of the EDF  $F_0(u, r)$ :

$$\begin{aligned} \frac{2e}{3m_e} \left[ \frac{1}{r} \frac{\partial}{\partial r} \left( r \frac{u^{3/2}}{\nu_m} \frac{\partial F_0}{\partial r} \right) - \frac{u^{3/2}}{\nu_m} \frac{1}{r} \frac{\partial}{\partial r} \left( r E_t \frac{\partial F_0}{\partial u} \right) \right] \\ + \frac{2e}{3m_e} \frac{\partial}{\partial u} \left[ -\frac{u^{3/2}}{\nu_m} E_t \frac{\partial F_0}{\partial r} + \frac{u^{3/2}}{\nu_m} (E_t^2 + E_z^2) \frac{\partial F_0}{\partial u} \right] \\ + \frac{\partial}{\partial u} \left( \frac{2m_e}{M_a} u^{3/2} \nu_m F_0 \right) = S(F_0). \quad (2) \end{aligned}$$

$F_0(u, r)$  is normalized to the electron density:  $n_e(r) = \int_0^\infty F_0(u, r) u^{1/2} du$ . The terms on the left hand side of

Eq. (2) describe in the order of their appearance the free diffusion of electrons, the counteracting mobility flow in the space charge field, the cooling and heating by the space charge field, the heating by the axial field, and the energy loss in elastic collisions. The right hand side accounts for the collision terms of the inelastic processes. The collision terms for excitation and superelastic processes read

$$\begin{aligned} S(F_0)_{exc, sup} = \sum_k \left( \nu_k(u) F_0(u, r) u^{1/2} \right. \\ \left. - \nu_k(u \pm u_k) F_0(u \pm u_k, r) (u \pm u_k)^{1/2} \right). \quad (3) \end{aligned}$$

Here  $\nu_k$  is the collision frequency of the  $k$ th inelastic process. The plus sign in Eq. (3) accounts for excitation collisions with a threshold energy  $u_k$ , while the minus sign applies for the related superelastic processes. The ionization can be included in the well-known approximation that the kinetic energy exceeding the ionization energy is distributed equally between the scattering and the released electron [28] ( $u_k^i$  is the ionization threshold energy):

$$\begin{aligned} S(F_0)_{ion} = \sum_k \left( \nu_k^i(u) F_0(u, r) u^{1/2} \right. \\ \left. - \nu_k^i(2u + u_k^i) F_0(2u + u_k^i, r) (2u + u_k^i)^{1/2} \right). \quad (4) \end{aligned}$$

The spatially dependent kinetic equation (2) represents an elliptic partial differential equation which can be solved numerically. However, for reasons of elucidating the physical nature of the problem and for numerical convenience it proved to be useful to introduce the *total energy*  $\varepsilon$  of electrons instead of the kinetic energy  $u$ . Thus the new variables are

$$r' = r, \quad (5)$$

$$\varepsilon = u - \Phi(r) = \frac{mv^2}{2e} - \Phi(r). \quad (6)$$

Using this set of new variables, one arrives at a diffusion type kinetic equation for the isotropic part of the EDF  $F_0(\varepsilon, r)$  [18,19]:

$$\begin{aligned} \frac{1}{r} \frac{\partial}{\partial r} \left( r u^{1/2} D_r(\varepsilon, r) \frac{\partial F_0(\varepsilon, r)}{\partial r} \right) \\ + \frac{\partial}{\partial \varepsilon} \left( u^{1/2} D_\varepsilon(\varepsilon, r) \frac{\partial F_0(\varepsilon, r)}{\partial \varepsilon} \right) = S(F_0). \quad (7) \end{aligned}$$

$u^{1/2} D_r(\varepsilon, r)$  and  $u^{1/2} D_\varepsilon(\varepsilon, r)$  can be considered as the coefficients for diffusion in configuration and in energy space [29], respectively, with

$$u^{1/2} D_r(\varepsilon, r) = \frac{2e}{3m} \frac{u(r)^{3/2}}{\nu_m(u)}, \quad (8)$$

$$u^{1/2} D_\varepsilon(\varepsilon, r) = \frac{2e}{3m} \frac{E_z^2}{\nu_m(u)} \frac{u(r)^{3/2}}{\nu_m(u)}. \quad (9)$$

Here the primes on the radial coordinate have been dropped for simplicity. It should be noted that the kinetic energy  $u$  is a function of the radial position now, since the total energy  $\varepsilon$  and  $r$  are considered as the independent variables. In the collision integral  $S(F_0)$  [Eqs. (3) and (4)]  $u$  has to be replaced by  $\varepsilon + \Phi(r)$  except for the arguments of  $F_0$ . The elastic collision term has been included in  $S(F_0)$  in Eq. (7).

The following considerations are limited to the case of an argon plasma for the moment. As cross section data, the momentum transfer cross section, a total excitation cross section, and the ionization cross section given by Krenz [30] have been used. Superelastic collisions have been neglected.

The physical processes governing the formation of the EDF can be qualitatively understood by the consideration of the kinetic equation (7) and the sketch of the range of integration in the total energy-radius domain in Fig. 1. The curved boundary  $\varepsilon = -\Phi(r)$  is the boundary where the kinetic energy is zero, i.e.,  $u(r) = 0$ . Excitation and ionization processes at a fixed position are possible if the kinetic energy exceeds the lowest threshold energy  $u_{ex}$ . Thus the domain where inelastic processes occur is bounded by the curve  $\varepsilon = -\Phi(r) + u_{ex}$  or  $u(r) = u_{ex}$ , i.e., by a curve defined as the space charge potential shifted about  $u_{ex}$ . If electrons entering this domain perform excitation or ionization processes, these processes can be interpreted as the absorption of high energy particles and the simultaneous emission of low energy particles. The formation of the EDF can be qualitatively understood as a diffusion process in energy and in coordinate space with a particle source at low energies and a sink in the absorption region at high energies. The absorption of high energy particles leads to a depletion of the EDF. Furthermore, close to the wall at total energies above the wall potential the EDF is depleted also by the outflow of electrons to the wall.

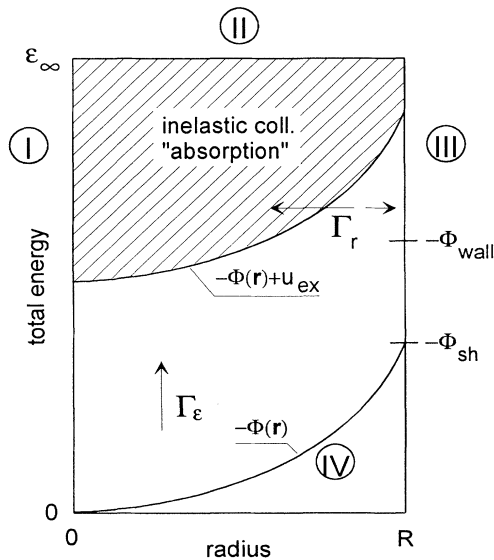


FIG. 1. Sketch of the domain of integration of the spatially dependent kinetic equation.

## B. Boundary conditions

The boundary conditions are a crucial aspect for the solution of this elliptic partial differential equation. The range of integration is depicted in Fig. 1. The slight disadvantage of the formulation in total energy for numerical purposes is that the domain of integration is not rectangular but possesses an irregular boundary defined by the space charge potential  $\varepsilon = -\Phi(r)$  or  $u(r) = 0$ . At each boundary a boundary condition has to be specified.

The boundary condition on the discharge axis (boundary I) is trivial, if radial symmetry of the problem is assumed:

$$\left. \frac{\partial F_0(\varepsilon, r)}{\partial r} \right|_{r=0} = 0. \quad (10)$$

For the boundary at the maximum total energy  $\varepsilon_\infty = 40$  V (boundary II) a von Neumann condition for the slope of the EDF has been specified. Considering the structure of the kinetic equation (7) in the inelastic energy range, it is obvious that an exponentially decreasing as well as an increasing solution are possible, where only the former is physically relevant. Assuming a reasonable slope of the solution at high energies is favorable for the isolation of the physically reasonable solution. Errors at this boundary can be interpreted as contributions of the undesired solution which are, however, exponentially damped towards low energies. Thus some rough estimate for the slope of the EDF has been used, which was obtained from Eq. (7) by neglecting the space dependence and assuming  $u(\varepsilon_\infty, r) \approx \varepsilon_\infty$ :

$$\left. \frac{\partial F_0(\varepsilon, r)}{\partial \varepsilon} \right|_{\varepsilon_\infty} = - \left( \frac{\nu^*(\varepsilon_\infty)}{D_\varepsilon(\varepsilon_\infty, r)} \right)^{1/2} F_0(\varepsilon_\infty, r), \quad (11)$$

where  $\nu^*$  is the total inelastic collision frequency. As a trial also the boundary condition  $F_0(\varepsilon_\infty, r) = 0$  has been used. The deviations between solutions obtained with both boundary conditions are negligible up to energies some volts less than  $\varepsilon_\infty$ , which evidences the exponential damping of the second solution.

At the wall (boundary III) the problem is considered up to the sheath boundary. The sheath itself is supposed to be infinitely thin, with its main physical characteristic being the potential drop within the sheath:  $\Phi_w - \Phi_{sh}$ , where  $\Phi_w$  is the wall potential. Electrons approaching the sheath boundary may have a total energy below or above the negative wall potential  $-\Phi_w$ . In the former case the electrons are reflected by the space charge potential in the sheath, so that the radial flux of electrons vanishes:

$$\left. \frac{\partial F_0}{\partial r} \right|_{r=R, \varepsilon \leq -\Phi_w} = 0. \quad (12)$$

Electrons with a total energy exceeding the wall potential may, in principle, be lost to the wall. However, for overcoming the potential drop within the sheath, the electrons must have a sufficient amount of kinetic energy perpendicular to the wall. This requirement defines a loss cone in velocity space [29]. An electron is able

to overcome the sheath potential if its velocity vector is inside the loss cone. Assuming that the EDF at the sheath boundary is still reasonably isotropic, the part of the chaotic flux of electrons which is lost to the wall (left hand side) has to be balanced by the radial flux of electrons (right hand side):

$$\left( vF_0(\varepsilon, r)u^{1/2} \frac{\delta\Omega}{4\pi} \right) \Big|_{r=R} = \left( -u^{1/2} D_r(\varepsilon, r) \frac{\partial F_0}{\partial r} \right) \Big|_{r=R}, \quad (13)$$

for  $\varepsilon > -\Phi_w$ . On the left hand side the fraction  $\delta\Omega/4\pi$  represents the fraction of lost thermal flux.  $\delta\Omega$  is the solid angle of the wall loss cone:

$$\delta\Omega = 2\pi \left( 1 - \sqrt{\frac{-\Phi_w + \Phi_{sh}}{\varepsilon + \Phi_{sh}}} \right). \quad (14)$$

It is derived by the simple consideration that the kinetic energy contained in the perpendicular velocity has to be at least equal to the sheath potential  $-(\Phi_w - \Phi_{sh})$ .

For the formulation of the fourth boundary condition at the curve  $u(r) = 0$  (boundary IV), consideration of the physical processes occurring at this boundary is necessary. If it is assumed that all processes which generate low energy electrons, like excitation and ionization, start with a zero cross section at their threshold, no electrons with exactly zero kinetic energy are created. If superelastic collisions obey the same threshold behavior, there is neither a source nor a sink of electrons along the boundary  $u(r) = 0$ . Considering the left hand side of Eq. (7) as the divergence of a diffusive flux in radius-total energy space, the absence of particle sinks or sources along the boundary requires the flux perpendicular to that boundary to be continuous. (The term perpendicular refers to normalized dimensionless variables, e.g.,  $r/R$  and  $\varepsilon/\varepsilon_\infty$ .) Since the flux of electrons from negative kinetic energies has to be zero, the flux normal to the curve  $u(r) = 0$  is zero. This leads to the following relation between the spatial and the energy flux components:

$$\left( -\frac{d\Phi(r)}{dr} D_r \frac{\partial F}{\partial r} \right) \Big|_{u=0} = \left( D_\varepsilon \frac{\partial F}{\partial \varepsilon} \right) \Big|_{u=0}, \quad (15)$$

or with  $E_t = -d\Phi/dr$

$$\left( -E_t \frac{\partial F}{\partial r} + E_z^2 \frac{\partial F}{\partial \varepsilon} \right) \Big|_{u=0} = 0. \quad (16)$$

### C. The nonlocal approach

An approximate and very efficient method for the solution of the above problem has been proposed by Bernstein and Holstein in 1954 [18] and Tsengin [19]. Their approach should be applicable in weakly collisional cases, namely, when the energy relaxation scale length  $\lambda_\varepsilon$  exceeds the typical inhomogeneity scale  $\Lambda$ :

$$\lambda_\varepsilon = \lambda \left( \frac{\nu_m}{\kappa\nu_m + \nu^*} \right)^{1/2} \gg \Lambda. \quad (17)$$

Here  $\lambda$  is the electron mean free path and  $\kappa = 2m_e/M_a$

is the fraction of kinetic energy transferred in elastic collisions. The basics of the nonlocal approach should only briefly be summarized here. For a detailed discussion the reader is referred to Refs. [18,19]. The nonlocal approach relies on three main ideas.

(1) The EDF is supposed to be a spatially homogeneous function of the total energy of the electrons up to a small first order correction:  $F_0(\varepsilon, r) = F_0^{(0)}(\varepsilon) + F_0^{(1)}(\varepsilon, r)$  with  $|F_0^{(1)}| \ll |F_0^{(0)}|$ . This assumption is quite obvious for the case when electrons are confined in a space charge potential and move without collisions and without heating (see Ref. [18]). Then the total energy is a constant of motion. This holds still in good approximation if  $\lambda_\varepsilon \gg \Lambda$ .

(2) The *spatially dependent* EDF of kinetic energy is obtained from a "modified Boltzmann relation"

$$F_0(u, r) = F_0^{(0)}(\varepsilon = u - \Phi(r)). \quad (18)$$

This relation means that for finding the EDF of kinetic energy the contribution of potential energy  $\varepsilon < -\Phi(r)$  is cut from  $F_0^{(0)}(\varepsilon)$  and the rest remains as the EDF of kinetic energy (see Ref. [23]).

(3) Since in the case  $\lambda_\varepsilon \gg \Lambda$  the spatial motion of electrons takes place on a much faster time scale than their "motion" in energy space, the EDF of total energy is obtained from a spatially averaged kinetic equation

$$\frac{\partial}{\partial \varepsilon} \left( \overline{u^{1/2} D_\varepsilon(\varepsilon, r)} \frac{\partial F_0^{(0)}(\varepsilon)}{\partial \varepsilon} \right) = \overline{S(F_0^{(0)})}. \quad (19)$$

The bars denote spatially averaged quantities [18,19] where the averages are defined by

$$\overline{G(\varepsilon, r)} = \frac{2}{R^2} \int_0^{r^*(\varepsilon)} G(\varepsilon, r) r dr. \quad (20)$$

$r^*(\varepsilon)$  denotes the turning point radius, defined by  $u(r^*(\varepsilon)) = 0$ . The spatial diffusion term in Eq. (7) drops out on spatial averaging. The averaged kinetic equation (19) is formally identical to the kinetic equation for a homogeneous plasma, which has been studied in a great number of investigations. In particular, a number of efficient numerical techniques are available for the solution of this equation.

The great advantage of the nonlocal approach is that the description of the spatially dependent electron kinetics is reduced to the solution of a one-dimensional, ordinary differential equation. A number of experimental studies has given qualitative evidence to the nonlocal approach [20–23]. In particular, points (1) and (2) have been convincingly demonstrated. However, to evidence the quantitative capabilities of this approach, it is necessary to prove that the spatially averaged kinetic equation (19) yields quantitatively the same results as the spatially dependent kinetic equation (7), within its range of applicability. This is our main aim in the discussion in Sec. IV.

### III. NUMERICAL METHOD

In order to solve the spatially dependent kinetic equation (7) numerically, the EDF  $F_0(\varepsilon, r)$  is represented by

discrete values on a grid in total energy-radius space. For each grid point the derivatives are represented by finite differences. For the solution of the resulting system of linear equations a multigrid algorithm has been used, which is described in detail by Hackbusch [31]. This scheme has been successfully applied to the solution of the Boltzmann equation in a planar geometry by Meijer *et al.* [16].

The resulting linear system of equations  $\mathcal{L} \cdot \mathbf{u} = \mathbf{f}$  can in principle be solved via a relaxation method like the Gauß-Seidel method. Here  $\mathcal{L}$  is the matrix of coefficients,  $\mathbf{u}$  the solution vector, and  $\mathbf{f}$  the inhomogeneity vector. However, this method is efficient in eliminating small scale deviations from the desired solution (high frequency components) but very inefficient to long scale deviations (low frequency components). The idea of the multigrid method is to make the deviation  $\mathbf{v} = \tilde{\mathbf{u}} - \mathbf{u}$  between a starting guess  $\tilde{\mathbf{u}}$  and the correct solution  $\mathbf{u}$  a smooth function by applying the Gauß-Seidel iteration as a smoothing procedure. The smoothed deviation  $\mathbf{v}$ , which is the correction to be applied to  $\tilde{\mathbf{u}}$ , can be better approximated on a coarser grid than the initial one. The equation which has to be solved for  $\mathbf{v}$  on the coarser grid is  $\mathcal{L} \cdot \mathbf{v} = \mathbf{d}$ , where  $\mathbf{d} = \mathcal{L} \cdot \tilde{\mathbf{u}} - \mathbf{f}$  is the defect. It is formally identical to the equation for  $\mathbf{u}$  on the higher level. Having found the correction  $\mathbf{v}$  on the coarser grid, it is extrapolated (prolongated) to the finer grid. The resulting high frequency errors can be efficiently eliminated by Gauß-Seidel smoothing. Since the equations which have to be solved for the solution  $\mathbf{u}$  on a higher level and  $\mathbf{v}$  on a lower level are equivalent, this scheme can be extended to include lower levels with coarser grids (multigrid scheme). The advantage of solving the problem on a hierarchy of fine and coarse grids is that a good reduction of low frequency errors is obtained by the solution on coarse grids while high frequency errors are eliminated by Gauß-Seidel smoothing on fine grids. Practically, the transition from a fine to a coarse grid is performed by halving the number of intervals in energy and radial direction.

The time required by this technique for the solution of the discretized Boltzmann equation for grid sizes up to  $513 \times 513$  points in the  $\epsilon$  and  $r$  directions, respectively, is of the order of less than one hour on a PC 486DX33. An accuracy of the discretized Boltzmann equation of about 0.01% is achieved. Good accuracies, however, can already be attained with grid sizes of  $65 \times 257$  points in the  $r$  and  $\epsilon$  directions, respectively, since the energy variation of the distribution function is much more pronounced than its variation with respect to the radius.

#### IV. RESULTS

In order to get an impression of the influence of the spatial inhomogeneity, in Fig. 2 EDF's of total energy are presented as a function of the radius for two neutral particle densities  $N_0$ . Note that the curved boundary corresponds to the boundary  $\epsilon = -\Phi(r)$  or  $u(r) = 0$  (cf. Fig. 1). This curve exactly represents the origins of the EDF's of kinetic energy in different radial positions. The

result for the lower pressure [Fig. 2(a)] obviously corresponds to the case of a spatially homogeneous EDF of total energy, which is addressed by the nonlocal approach. It should be stressed again that the EDF's of kinetic energy are far from being radially constant. For the higher neutral density in Fig. 2(b) the EDF reveals strong deviations from the spatial homogeneity, in particular, in the energy range where inelastic collisions occur. A strong depletion of the EDF towards the center of the discharge is observed. This decrease of the EDF is an effect which is caused by inelastic collisions. For a given total energy,

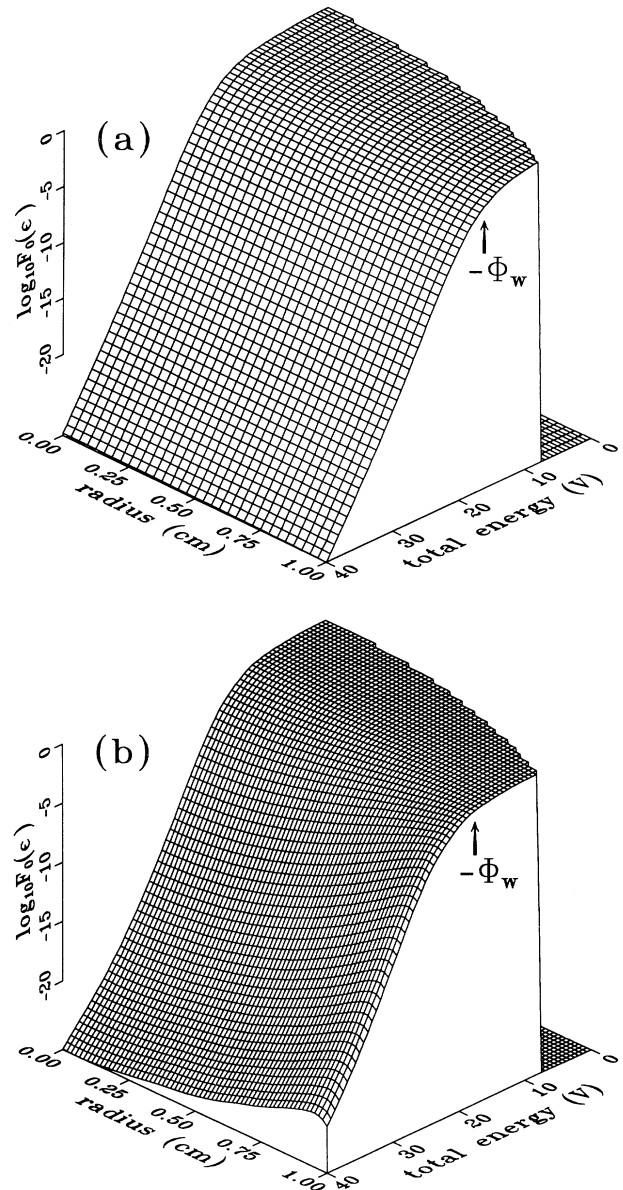


FIG. 2. Solutions of the spatially dependent kinetic equation: (a)  $N_0 = 3 \times 10^{21} \text{ m}^{-3}$ , showing explicitly a nonlocal behavior, and (b)  $N_0 = 3 \times 10^{23} \text{ m}^{-3}$ , revealing a depletion of the EDF in the center due to inelastic collisions and at the sheath boundary due to the electron drain to the wall. ( $E_z/N_0 = 25 \times 10^{-21} \text{ V m}^2$ .)

the kinetic energy is maximal in the center and thus also the efficiency of inelastic collisions. For total energies only slightly exceeding the excitation threshold of argon at 11.55 eV even the following situation is possible. While electrons in the center of the discharge are already capable of performing inelastic processes, electrons with the same total energy but close to the wall have a too small kinetic energy to perform excitation. Thus the boundary between the elastic and inelastic range of the EDF reflects the shape of the excitation region in Fig. 1. In the weakly collisional case in Fig. 2(a) these differences are leveled by the fast spatial redistribution. A second drop of the EDF close to the wall is visible for energies above the wall potential. It is caused by the losses of electrons to the wall. The drop of the EDF increases with growing energy, since the loss cone angle increases, too. It should be mentioned that the solutions presented here are not really stationary solutions, since the electric field is not specified self-consistently and an outflow of electrons to the walls is permitted. In the following the radial outflow of electrons has been suppressed by setting  $-\Phi_w = \varepsilon_\infty$  and the generation of secondary electrons by ionization has been neglected so that stationary solutions are discussed.

The nonlocal behavior of the EDF in Fig. 2(a) has an interesting consequence for the mean kinetic energy of the EDF's. Since in the nonlocal regime the EDF is a spatially homogeneous function of total energy and the EDF of kinetic energy is found by cutting the first part corresponding to the potential energy from  $F_0^{(0)}(\varepsilon)$ , the inelastic range starts at lower and lower kinetic energies when the wall is approached. This results in a drop of the mean kinetic energy from the center towards the wall as shown in Fig. 3. For higher neutral densities this effect is less pronounced. In these cases the EDF approaches the "local" regime, where the EDF is in equilibrium with the local electric field strength and effects of spatial inhomogeneity become more and more unimportant. It should be mentioned that the above argument applies only to convex EDF's (dc case, rarer gases), i.e., to EDF's for

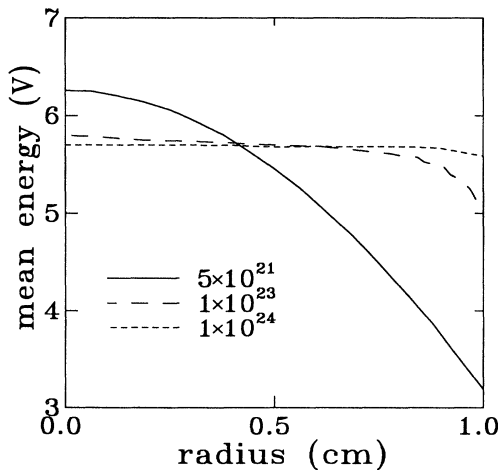


FIG. 3. Mean kinetic energies of the solutions of the spatially dependent kinetic equation. ( $E_z/N_0 = 25 \times 10^{-21} \text{ V m}^2$ .)

which  $T_e = (d \ln F_0 / d\varepsilon)^{-1}$  decreases with growing energy. In hf plasmas concave EDF's can be found which are characterized by a strong group of low energy electrons with a low "temperature" [32]. The removal of this low temperature group can even lead to the reverse effect of an increase of the mean kinetic energy towards the wall [22,23].

Up to now the discussion has been more or less qualitative. To give a quantitative comparison between the results of the numerical solution of the complete kinetic equation (7) and those obtained from the spatially averaged equation (19), EDF's are calculated from both approaches for various neutral-species densities  $N_0$  at constant  $E_z/N_0$ . The EDF's obtained from the spatially averaged equation (19) depend only on  $E_z/N_0$  so that the same result applies to all neutral-species densities. The results of the spatially dependent kinetic equation differ due to the differences in the radial transport. Figure 4 demonstrates a good quantitative agreement between the result of the nonlocal approach and the solution of the more general equation for neutral particle densities up to  $N_0 = 5 \times 10^{21} \text{ m}^{-3}$ . This result proves that the nonlocal approach is not only useful for qualitative explanations

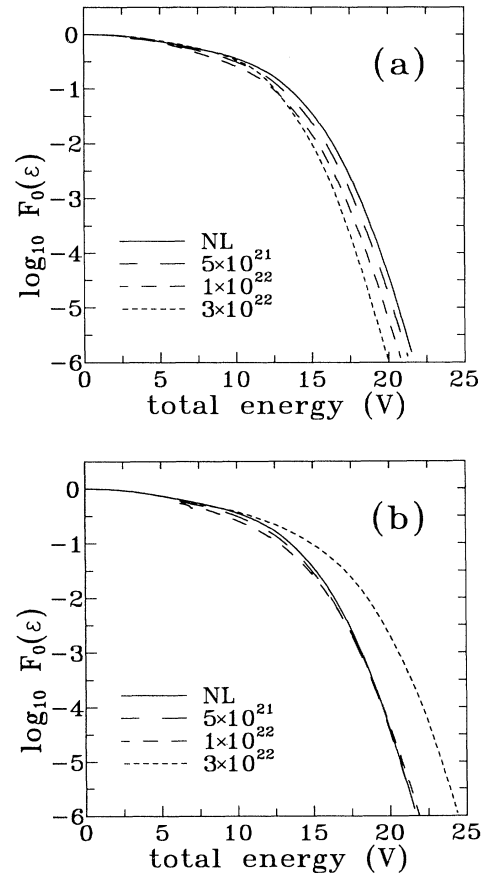


FIG. 4. Comparison of the solutions of the complete kinetic equation to the EDF resulting from the nonlocal approach (NL) (a) in the center, (b) close to the wall ( $r = 0.9R$ ). The normalized field strength is kept constant,  $E_z/N_0 = 25 \times 10^{-21} \text{ V m}^2$ , and the radius is  $R = 1 \text{ cm}$ .

but is really capable of yielding quantitative predictions. For higher neutral densities the deviations, which have already been discussed above, start to build up. The solution of the complete kinetic equation exceeds the nonlocal EDF at the wall, while it is more strongly depleted in the center.

The macroscopic properties of the discharge, in particular, the electron density profile, are most sensitively affected by the ionization profile. Thus to judge the quantitative accuracy obtained by the nonlocal approach, it seems to be reasonable to compare the ground state ionization frequencies obtained by this method to those from the solution of the spatially dependent kinetic equation (7). This comparison is presented in Table I. It is obvious that for neutral-species densities up to  $3 \times 10^{21} \text{ m}^{-3}$  deviations between the ionization frequencies of the two approaches are of about 30%. If one keeps in mind that the typical accuracy of experimentally determined ionization cross sections is of the same order, this seems to be a reasonable accuracy for a kinetic approach. Figure 5(a) shows the corresponding energy relaxation lengths for constant kinetic energy which are of course energy dependent. In order to determine the ionization frequency with an accuracy of a few percent in argon the energy range up to about 20 eV is of interest. For  $N_0 = 3 \times 10^{21} \text{ m}^{-3}$  the energy relaxation length (for a fixed kinetic energy) is almost equal to the tube radius. Thus on the first view the condition  $\lambda_\epsilon(u) \approx R$  is sufficient to obtain the above 30% accuracy of the EDF by the nonlocal approach. However, it is more appropriate but also more difficult to consider a cross section averaged energy relaxation length, since during the electrons' motion across the discharge the kinetic energy is not constant. The exact cross section averaged energy relaxation length thus depends also on the exact shape of the space charge potential. For the potential used in this investigation one obtains the energy relaxation lengths shown in Fig. 5(b). For  $N_0 = 3 \times 10^{21} \text{ m}^{-3}$   $\bar{\lambda}_\epsilon(\bar{\epsilon}) \gtrsim 3R$  holds over the interesting energy range. Since the cross section averaged energy relaxation length requires the knowledge of the potential it may be more convenient to consider the non-averaged  $\lambda_\epsilon(u)$ . Here the condition  $\lambda_\epsilon(u) \approx R$  can serve as a rough guide for the upper limit of applicability of the nonlocal approach.

Finally, it should be mentioned that deviations from the spatial homogeneity of the EDF of total energy may

TABLE I. Ratios  $\nu_{i,nl}/\nu_{i,ke}$  of ionization frequencies in the center obtained from the nonlocal approach (subscript *nl*) to those from the solution of the spatially dependent kinetic equation (subscript *ke*) for different neutral densities  $N_0$  and normalized field strengths  $E_z/N_0$ .

$N_0 \text{ (m}^{-3}\text{)}$ \backslash $E_z/N_0 \text{ (10}^{-21} \text{ V m}^{-2}\text{)}$	12.5	25.0	37.5
$1 \times 10^{21}$	1.04	1.06	1.06
$3 \times 10^{21}$	1.29	1.32	1.34
$1 \times 10^{22}$	1.77	1.92	1.98
$3 \times 10^{22}$	8.21	9.62	7.44
$1 \times 10^{23}$	145.13	34.28	14.65

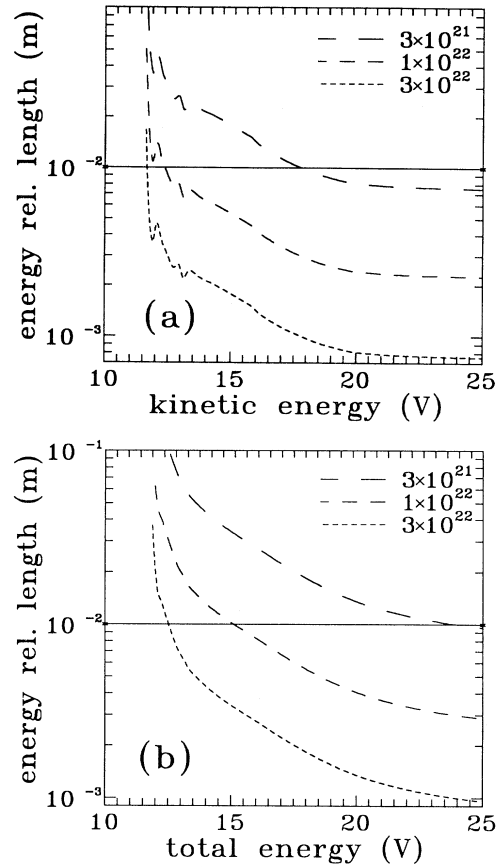


FIG. 5. The energy dependence of the energy relaxation length: (a) for fixed kinetic energy, and (b) for constant total energy and averaged over the discharge cross section.

not only be caused by collisional effects but also be due to an inhomogeneity of the axial electric field. Such an effect may be important for microwave or rf plasmas where frequently very inhomogeneous electric field distributions are found. To study this effect, a radial profile of the axial field has been assumed:  $E_z(r) = E_{z,0}[1 + \beta(r/R)^2]$ . (Such a profile is, of course, not realistic for a positive column,

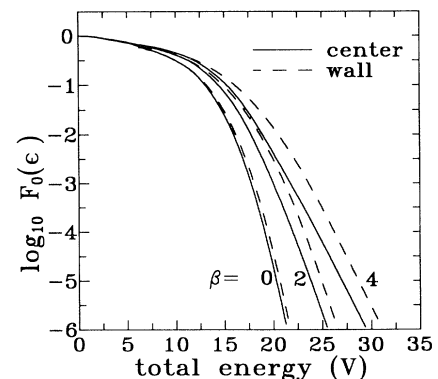


FIG. 6. Influence of the radial inhomogeneity of the axial electric field for  $N_0 = 5 \times 10^{21} \text{ m}^{-3}$  and a field profile  $E_z(r) = E_{z,0}[1 + \beta(r/R)^2]$  with  $R=1 \text{ cm}$ . ( $E_{z,0}/N_0 = 25 \times 10^{-21} \text{ V m}^{-2}$ .)

but may similarly be found, for instance, in overdense microwave discharges.) In Fig. 6 the EDF's in the center and close to the wall are given for a neutral-species density of  $N_0 = 5 \times 10^{21} \text{ m}^{-3}$  and different  $\beta$ . While for  $\beta = 0$  the EDF's in the center and close to the wall almost coincide (nonlocal case) some deviations build up for increasing  $\beta$ . However, even for  $\beta = 4$  the deviations are comparatively small so that the nonlocal approach is still a good approximation. It should be noted that in the local limit, i.e., when the EDF is assumed to be in equilibrium with the local electric field, this radial increase of the electric field would have produced drastically different EDF's. Thus the radial redistribution of energy due to the spatial motion of electrons is still a very important process in the considered case.

### V. SUMMARY AND CONCLUSIONS

We have presented the numerical solution of the spatially dependent kinetic equation for the isotropic part of the EDF obtained within the two-term approximation. Comparisons with results of the nonlocal approach yield a good quantitative agreement for neutral-species densities up to about  $N_0 = 3 \times 10^{21} \text{ m}^{-3}$  at  $R=1 \text{ cm}$  in argon. The deviations of the ionization frequencies are of the order of 30% at this neutral-species density. As a rough estimate for the upper limit of the range of applicability the condition  $\lambda_e(u) \approx R$  (for the interesting energy range) can be employed. It has been shown that a spatially inhomogeneous maintaining electric field favors deviations from the spatial constancy of the EDF of total energy. However, these deviations are much less pronounced than have to be expected from a local model, where the EDF is assumed to be in equilibrium with the local electric field.

It should once again be pointed out that within its range of applicability the nonlocal approach is an extremely valuable tool for the description of the spatially dependent electron kinetics. Regardless of the number of spatial dimensions to be considered, the electron kinetics

is reduced to a one-dimensional problem in total energy space. By the use of the nonlocal approach highly efficient kinetic models can be developed. Recently it has been exemplified by a spatially two-dimensional kinetic model for an inductively coupled rf discharge which can be easily solved on a PC486 computer within one hour [26].

The great value of the nonlocal approach for efficient plasma modeling makes further investigations necessary. Thus the range of applicability should be investigated for molecular gases which are interesting for many applications. In these gases vibrational excitation with low threshold energies may restrict the range of applicability of the nonlocal approach to much lower neutral-species densities than in rare gases. Furthermore, the transition to the local regime should also be investigated in future studies. At high neutral-species densities, when the energy relaxation length is much smaller than the typical inhomogeneity scale over the whole energy range of the EDF, the EDF should be in equilibrium with the local electric field and the spatial inhomogeneity should become unimportant. Under these conditions the EDF could be obtained via solution of the kinetic equation for a homogeneous plasma using the local electric field strength, which again is a one-dimensional ordinary differential equation. Thus it may be possible to use simplified approaches in the weakly as well as in the highly collisional case. In the intermediate range of neutral-species densities probably the solution of the spatially dependent kinetic equation as presented here remains the appropriate method to describe the spatially dependent electron kinetics.

### ACKNOWLEDGMENTS

The authors are indebted to Professor H. Schlüter, Professor L. D. Tsendin, Professor C. M. Ferreira, Professor R. Winkler, Dr. D. Uhrlandt, and to Dr. L. L. Alves for valuable discussions. This work was supported by the Deutsche Forschungsgemeinschaft (SFB 191).

- 
- [1] G. G. Lister, *J. Phys. D* **25**, 1649 (1992).
  - [2] T. J. Sommerer and M. J. Kushner, *J. Appl. Phys.* **71**, 1654 (1992).
  - [3] P. L. G. Ventzek, T. J. Sommerer, R. J. Hoekstra, and M. J. Kushner, *Appl. Phys. Lett.* **63**, 605 (1993).
  - [4] P. L. G. Ventzek, R. J. Hoekstra, and M. J. Kushner, *J. Vac. Sci. Technol. B* **12**, 461 (1994).
  - [5] M. Surendra and D. B. Graves, *IEEE Trans. Plasma Sci.* **19**, 144 (1991).
  - [6] V. Vahedi, C. K. Birdsall, M. A. Liebermann, G. DiPeso, and T. D. Rognlien, *Phys. Fluids B* **5**, 2719 (1993).
  - [7] V. Vahedi, G. DiPeso, C. K. Birdsall, M. A. Liebermann, and T. D. Rognlien, *Plasma Sources Sci. Technol.* **2**, 261 (1993).
  - [8] W. N. G. Hitchon, G. J. Parker, and J. E. Lawler, *IEEE Trans. Plasma Sci.* **21**, 228 (1993).
  - [9] M. J. Kushner, *J. Appl. Phys.* **54**, 4958 (1983).
  - [10] W. N. G. Hitchon, D. J. Koch, and J. B. Adams, *J. Comput. Phys.* **83**, 79 (1989).
  - [11] T. J. Sommerer, W. N. G. Hitchon, and J. E. Lawler, *Phys. Rev. Lett.* **63**, 2361 (1989).
  - [12] T. J. Sommerer, W. N. G. Hitchon, and J. E. Lawler, *Phys. Rev. A* **39**, 6356 (1989).
  - [13] L. C. Pitchford and A. V. Phelps, *Phys. Rev. A* **25**, 540 (1982).
  - [14] R. Winkler, H. Deutsch, J. Wilhelm, and C. Wilke, *Beitr. Plasmaphys.* **24**, 285 (1984).
  - [15] V. A. Feoktistov, A. M. Popov, O. B. Popovicheva, A. T. Rakhimov, T. V. Rakhimova, and E. A. Volkova, *IEEE Trans. Plasma Sci.* **19**, 163 (1991).
  - [16] P. M. Meijer, W. J. Goedheer, and J. D. P. Passchier, *Phys. Rev. A* **45**, 1098 (1992).
  - [17] M. J. Hartig and M. J. Kushner, *J. Appl. Phys.* **73**, 1080 (1993).
  - [18] I. B. Bernstein and T. Holstein, *Phys. Rev.* **94**, 1475 (1954).
  - [19] L. D. Tsendin, *Zh. Eksp. Teor. Fiz.* **66**, 1638 (1974) [*Sov. Phys. JETP* **39**, 805 (1974)].



- [20] K. Wiesemann, *Ann. Phys. (Leipzig)* **23**, 275 (1969).
- [21] D. Herrmann, A. Rutscher, and S. Pfau, *Beitr. Plasma-phys.* **10**, 75 (1970).
- [22] V. A. Godyak and R. B. Piejak, *Appl. Phys. Lett.* **63**, 3137 (1993).
- [23] U. Kortshagen, *Phys. Rev. E* **49**, 4369 (1994).
- [24] I. D. Kaganovich and L. D. Tsendin, *IEEE Trans. Plasma Sci.* **20**, 66 (1992).
- [25] U. Kortshagen, I. Pukropski, and M. Zethoff, *J. Appl. Phys.* **76**, 2048 (1994).
- [26] U. Kortshagen and L. D. Tsendin, *Appl. Phys. Lett.* **65**, 1355 (1994).
- [27] I. P. Shkarofsky, T. W. Johnston, and M. P. Bachynski, *The Particle Kinetics of Plasmas* (Addison-Wesley, Reading, MA, 1966).
- [28] S. Yoshida, A. V. Phelps, and L. C. Pitchford, *Phys. Rev. A* **27**, 2858 (1983).
- [29] L. D. Tsendin and Y. B. Golubovskii, *Zh. Tekh. Fiz.* **47**, 1839 (1977) [*Sov. Phys. Tech. Phys.* **22**, 1066 (1977)].
- [30] J. Krenz, University of Hanover, technical report (unpublished).
- [31] W. Hackbusch, *Multi-Grid Methods and Applications* (Springer, Berlin, 1985).
- [32] V. A. Godyak, R. B. Piejak, and B. M. Alexandrovich, *Plasma Sources Sci. Technol.* **1**, 36 (1992).